LA-UR- 972308

Approved for public release; distribution is unlimited.

Title: EXPERIMENTAL RESULTS COMPARING PULSED CORONA AND DIELECTRIC BARRIER DISCHARGES FOR POLLUTION CONTROL (Paper)

Author(s): Richard A. Korzekwa, Louis A. Rosocha, and Z. Falkenstein
CST-18

Submitted to: Eleventh IEEE International Pulsed Power Conference
June 29 - July 2, 1997
Baltimore, Maryland

Los Alamos
NATIONAL LABORATORY

REPORT DOCUMENTATION PAGE

Form Approved
OMB No. 074-0188

1. AGENCY USE ONLY (Leave blank)	2. REPORT DATE	3. REPORT TYPE AND DATES COVERED
	June 29, 1997	

4. TITLE AND SUBTITLE
Experimental Results Comparing Pulsed Corona and Dieclectric Barrier Discharges for Pollution Control (Paper)

5. FUNDING NUMBERS
N/A

6. AUTHOR(S)
Richard A. Korzekwa, Louis A. Rosocha, Z. Falkenstein

7. PERFORMING ORGANIZATION NAME(S) AND ADDRESS(ES)
Los Alamos National Laboratory

8. PERFORMING ORGANIZATION REPORT NUMBER
LA-UR-972308

9. SPONSORING / MONITORING AGENCY NAME(S) AND ADDRESS(ES)
SERDP
901 North Stuart St. Suite 303
Arlington, VA 22203

10. SPONSORING / MONITORING AGENCY REPORT NUMBER
N/A

11. SUPPLEMENTARY NOTES
Submitted to: Eleventh IEEE International Pulsed Power Conference, June 29 - July 2, 1997, Baltimore, MD.

12a. DISTRIBUTION / AVAILABILITY STATEMENT
Approved for public release: distribution is unlimited.

12b. DISTRIBUTION CODE
A

13. ABSTRACT ***(Maximum 200 Words)***

Nonthermal Plasmas efficiently produce highly reactive chemical species for the destruction of pollutants in gaseous effluents. Two devices commonly used to produce a nonthermal plasma in atmospheric pressure gases are the pulsed corona reactor (PCR) and the dielectric barrier discharge reactro, also referred to as a "silent discharge plasma" (SDP) reactor. The PCR produces a nonthermal plasma by applying a fast-rising, short duration, high-voltage pulse to a coaxial wire/tube geometry which initiates multiple streamers (electron avalanches) along the length of the tube. The high-energy electrons produced in the streamers create the desired active species while maintaining near ambien neutral gas temperatures. The streamers are extinguished as the energy is depleted in the storage capacitance. The SDP reactor is construced using either a coaxial or flat-plate electrode geometry with at least one dielectric barrier placed between the high-voltage electrodes, leaving a few mm gap in which the nonthermal plasma is generated. When the breakdown voltage is reached in the gas gap, microdischarge streamers are produced throughout the gap volume wich self-terminate when the build up of surface charge on the dielectric reduces the electric field in the gap. A comparison of the results obtained in these devices is presented for various operating conditions and gas pollutants. Our primary interest is to explore whether the added complexity of fast risetime circuits has a payoff in terms of overall chemical-processing efficiency.

14. SUBJECT TERMS
pulsed corona reactor; PCR; silent discharge plasma; nonthermal plasma; NTP; SDP; SERDP; SERPD Collection

15. NUMBER OF PAGES
7

16. PRICE CODE N/A

17. SECURITY CLASSIFICATION OF REPORT	18. SECURITY CLASSIFICATION OF THIS PAGE	19. SECURITY CLASSIFICATION OF ABSTRACT	20. LIMITATION OF ABSTRACT
unclass.	unclass.	unclass.	UL

EXPERIMENTAL RESULTS COMPARING PULSED CORONA AND DIELECTRIC BARRIER DISCHARGES FOR POLLUTION CONTROL

R. Korzekwa, L. Rosocha, and Z. Falkenstein
Los Alamos National Laboratory
P.O. Box 1663, E-525
Los Alamos, NM 87545

ABSTRACT - Nonthermal plasmas efficiently produce highly reactive chemical species for the destruction of pollutants in gaseous effluents. Two devices commonly used to produce a nonthermal plasma in atmospheric pressure gases are the pulsed corona reactor (PCR) and the dielectric barrier discharge reactor, also referred to as a "silent discharge plasma" (SDP) reactor. The PCR produces a nonthermal plasma by applying a fast-rising, short duration, high-voltage pulse to a coaxial wire/tube geometry which initiates multiple streamers (electron avalanches) along the length of the tube. The high-energy electrons produced in the streamers create the desired active species (e.g., radicals) while maintaining near ambient neutral gas temperatures. The streamers are extinguished as the energy is depleted in the storage capacitance. The SDP reactor is constructed using either a coaxial or flat-plate electrode geometry with a least one dielectric barrier placed between the high-voltage electrodes, leaving a few millimeter gap in which the nonthermal plasma is generated. When the breakdown voltage is reached in the gas gap, microdischarge streamers are produced throughout the gap volume which self-terminate when the build up of surface charge on the dielectric reduces the electric field in the gap. Although a fast rising pulse can be used to drive an SDP reactor, a sinusoidal voltage with a frequency of a few kilohertz is typically used to drive this type of reactor. When a fast-rising voltage pulse is used to drive these reactors, a higher reduced electric field strength (E/N) can be obtained than in the low-frequency-driven SDP reactors. In many cases a higher E/N results in a more efficient production of chemical radicals, which in turn interact with and destroy the low concentration pollutants in the gas. Commercially available power supplies are commonly used to drive the low frequency SDP reactor systems. These provide a simple and robust method of producing a nonthermal plasma for high power applications without the complexity of fast risetime, high-voltage switching circuits. A comparison of the results obtained in these devices is presented for various operating conditions and gas pollutants. Our primary interest is to explore whether the added complexity of fast risetime circuits has a payoff in terms of overall chemical-processing efficiency.

INTRODUCTION

The use of nonthermal plasmas for the destruction of hazardous gas pollutants has been investigated in recent years[1,2]. Two of the most common high-voltage discharge techniques used to produce a nonthermal plasma are the dielectric-barrier and the pulsed corona discharges. The most often used method of driving a dielectric-barrier discharge is with a low-frequency (few kilohertz) ac power source and a high-voltage step up transformer. Self-extinguishing microdischarges lasting a few to tens of nanoseconds are produced in a gas gap of a few millimeters between dielectric sheets (or tubes) with electrodes on either side. Most pulsed corona discharges are driven with high-voltage pulses with risetimes of 10 ns or greater and pulse widths of tens of nanoseconds to a few hundred nanoseconds. Typical corona wire sizes range from a fraction to a few millimeters with outer conducting tubes of various sizes. Multiple simultaneous streamers are formed along the length of the discharge tube, on the order of tens per centimeter[3]. A dielectric-barrier discharge can also be driven with a fast pulse high-voltage circuit. Compared to a low-frequency driven dielectric barrier-discharge a fast pulsed nonthermal discharge has a much higher breakdown electric field. A comparison has been made of the removal efficiency of various volatile organic compounds (VOC's) in dry air using these different methods of producing a nonthermal discharge.

EXPERIMENTAL DESCRIPTIONS

The pulsed positive corona setup is shown in Fig. 1. A constant current power supply, EMI model 500-40KV-POS, is used to charge a storage capacitor, C_{sp}, with a repetition frequency set by the control module. When the breakdown voltage of the coaxial self-breaking hydrogen-filled spark gap is reached, a high voltage pulse is delivered to the reactor tube capacitance, C_{pcr}, through the stray inductance, L_s. When the corona inception voltage is reached at the reactor tube, multiple simultaneous streamer discharges, represented by a time varying resistance R_d, are produced in the tube. A coaxial capacitive voltage divider, V_{pcr} with a sensitivity of 2.5×10^{-4} V/V, capable of measuring nanosecond risetime pulses with pulsewidths less than 150 ns was constructed at the input to the tube. The pulsed corona current was measured using a current viewing resistor, R_{cvr}, and was also constructed at the reactor input. This probe was capable of measuring nanosecond risetime pulses with a sensitivity of 20 A/V. The power dissipated in the discharge was determined using these probes. A feedback signal from the current probe (used as an indicator of when the spark gap closed) was sent to the control module to inhibit the power supply. The pulsed corona reactor tube was constructed using a stainless steel corona wire with a diameter of 500 μm, and stainless steel tubing as the outer conductor with an inner diameter of 2.5 cm. The length of the tube was 90 cm. A high-voltage alumina feedthrough was constructed at one end to apply the pulse to the wire and another alumina insulator was used to support the other end of the wire. The gas flow is introduced into the tube through SWAGELOK gas fittings at the gas manifolds at each end. This reactor design could be used up to temperatures of 700 C. For C_{sp} = 126 pF, L_s = 400 nH, and C_{pcr} = 25 pF, the waveforms in Fig. 2 were obtained showing the voltage and current of a typical corona pulse in room temperature dry air. The energy per pulse dissipated in the discharge was approximately 60 mJ. The system could be operated at a repetition frequency greater than 1 kHz with peak output voltages of up to 30 kV.

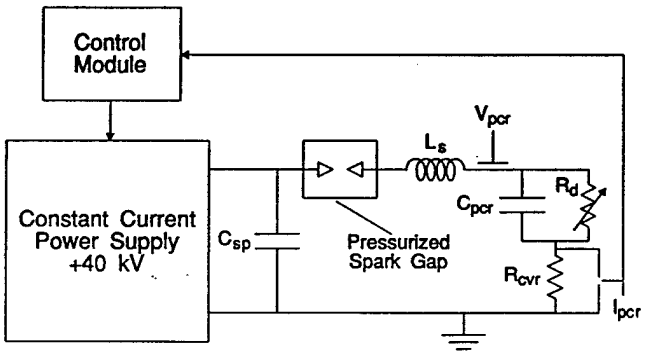

Figure 1. The equivalent circuit for the pulsed corona system setup.

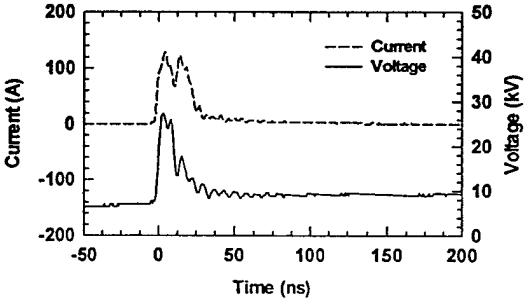

Figure 2. Typical pulsed corona current and voltage pulses versus time.

A diagram of the ac-driven dielectric-barrier discharge system is shown in Fig. 3. A variable frequency, 3 kW, ac power supply (Elgar model 3001-165A) was used to drive a high-voltage step up transformer (Stangenes Model SI-8020) which supplied power to the dielectric-barrier discharge cell. The operating frequency was 1.2 kHz with variable discharge powers up to 350 W. The discharge cell was constructed in a flat-plate geometry using two 0.3 cm x 38 cm x 70 cm Pyrex plates with a gap spacing of 3.5 mm and an active discharge area of 1800 cm^2. Two aluminum electrode plates were pressed to each side of the cell with a charge measuring capacitor, C_Q, between the low voltage plate and ground. The high-voltage transformer is connected to ground and the high-voltage electrode plate and a high-voltage probe (Tektronix model P6015A) was used to measure the voltage across the cell, V_{cell}. The energy per cycle in the discharge is obtained by plotting the charge driven through the cell versus the voltage across the cell for one cycle and calculating the area of the resulting parallelogram, shown in Fig. 4. The power in the cell is then found by multiplying the energy per cycle by the operating frequency.

A fast risetime pulse generator has been developed to drive a small dielectric-barrier discharge. A circuit diagram of the thyratron switched pulse circuit and discharge cell is shown in Fig. 5.

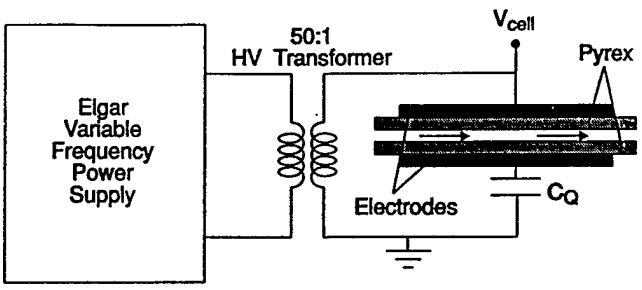

Figure 3. The ac-driven dielectric-barrier setup.

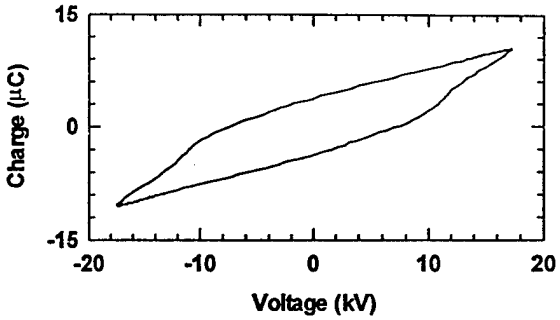

Figure 4. The charge versus voltage for the ac-driven dielectric-barrier discharge.

A storage capacitor, C_{st} = 1.2 nF, was charged from a positive dc high-voltage power supply through a charging resistor, R_{ct}. A fast risetime thyratron (EEV CX1588) was used to switch the positive side of C_{st} to ground producing a negative high-voltage pulse. An inductance, L_r, was used to allow the dc charging of C_{st} and to act as a high impedance to the fast pulse enabling the pulse to be delivered to the cell and to the stray high-voltage cable capacitance, C_c = 150 pF. The combination of L_r and the resistor, R_r, is also used to "ringout" the residual voltage left on the circuit, after the microdischarge has occurred, to enable the system to be charged and triggered again at the desired repetition frequency. A high-voltage probe (Tektronix model P6015A) and a current transformer (Pearson model 2877) were used to measure the voltage across and the current through the dielectric barrier discharge cell to obtain the dissipated energy per pulse in the cell. The risetime was limited by the stray inductance, L_{st}, and C_c. The pulsed dielectric-barrier system can be operated at peak voltages of up to 40 kV, a risetime of 6 ns, repetition rates of up to 20 Hz, and a temporal jitter of 4 ns. A single-barrier discharge cell, with a fixed gap spacing of 2 mm, is also shown in Fig. 5. The dielectric barrier is a 3-mm thick Pyrex plate which covers a 3.8-cm diameter high-voltage electrode. The lower stainless steel electrode was 2.54 cm in diameter. The cell was placed in an aluminum enclosure, with gas ports and a high-voltage feedthrough, to reduce the inductance at the cell and provide electromagnetic shielding. Typical voltage and current waveforms are shown in Fig. 6 for a discharge in dry air. The microdischarge occurs at the large negative peak on the current waveform.

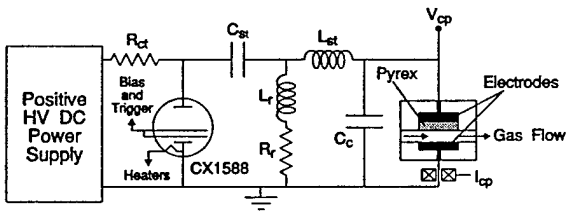

Figure 5. The equivalent circuit and reactor for the pulsed dielectric-barrier setup.

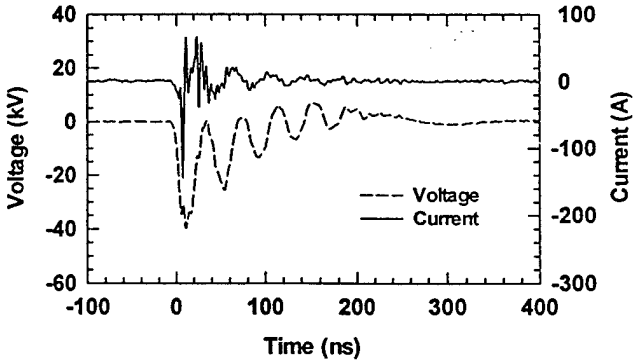

Figure 6. The voltage and current versus time for pulsed dielectric-barrier discharge.

A gas bottle was filled to a high pressure with a mixture of dry air and the desired VOC concentration. A gas regulator and mass flow controller were used to set the flow through the discharge tube or cell before entering the vent. Two methods were used to measure the VOC reduction, 1) a gas-chromatograph/mass-spectrometer, GC/MS, (HP model 5890 GC and HP model 5972 MS) was connected directly to the output line of the discharge volume and 2) a gas-tight syringe was used to extract a sample at a known volume from the gas output line which was then injected into a gas chromatograph with a sample concentrator (Varian model Star 3400CX GC and OI Corp. model 4460A

sample concentrator). The data for the ac-driven dielectric-barrier discharge was obtained using the GC/MS and the data for the pulsed discharges was obtained using the GC with a sample concentrator.

EXPERIMENTAL RESULTS

The removal of three compounds (trichloroethylene-TCE, methyl ethyl ketone-MEK, and methylene chloride-MeCl) has been measured using these devices. The removal is defined as $[X]/[X]_o$, where $[X]_o$ is the initial concentration and [X] is the final concentration in units of ppmv. The removal is plotted as a function of plasma energy deposited into the gas or specific energy, **E** in units of J/l.

The first measurements were made using all three compounds, seperately, to compare the pulsed corona and ac-driven dielectric-barrier discharges at room temperature. Figure 7 shows the removal versus **E** for 200 ppm of TCE, where there is no noticeable difference in the removal efficiency for energy densities up to 400 J/l between these two types of discharges. A double-exponential curve fit is also plotted which shows a slight divergence from a single-exponential fit (a straight line) indicating other than first order reactions at the higher energy densities. A double-exponential curve fit applies to all of the removal data presented. A similar plot for 1000 ppm of MEK is shown in Fig. 8, where for energy densities up to 1500 J/l there is no distinguishable difference in removal efficiency. However, for higher energy densities there is a slight difference attributed to a change in gas temperature which will be discussed in another section. In Fig. 9, the removal efficiency is plotted for 1000 ppm MeCl, where for low energy densities up to 1 kJ/l, there is good agreement between the pulsed corona and dielectric-barrier discharges, but for high energy densities the pulsed corona discharge has a significantly better removal efficiency. Because of this difference at high energy densities, the temperature was measured on the outer surface of the pulsed corona tube with the values given in Fig. 9. The difference in removal efficiency can be attributed to this increase in temperature. The removal efficiencies were also independent of concentration for 100-200 ppm of TCE and for 200-1000 ppm of MeCl.

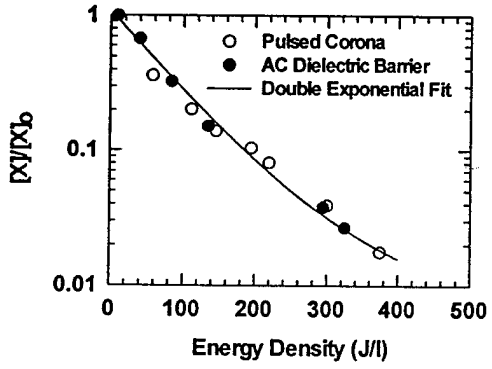

Figure 7. The removal versus energy density for 200 ppm of TCE in dry air.

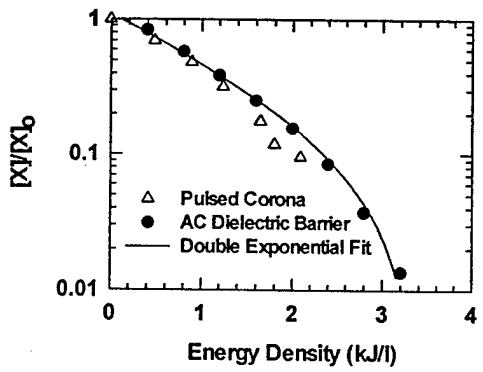

Figure 8. The removal versus energy density for 1000 ppm of MEK in dry air.

A comparison of the removal efficiency for the ac-driven and pulsed dielectric-barrier discharges was also obtained for 200 ppm of TCE in dry air. As seen in Fig. 10, the removal efficiencies, again, were similar for energy densities up to 200 J/l. This indicates that the effect of an increased breakdown field produced by pulsed discharges does not affect the removal efficiency for TCE in dry air.

Depending on the compound to be treated and the reaction chemistry, the removal efficiency can be greatly affected by temperature. The temperature dependence of the reaction kinetics has the form $k = A \exp(-T_A/T)$, where k is the rate constant in units of cm^3/molecule-s, A is the preexponential factor with the same units as k, and T_A is the activation energy in units of temperature (in K). For reactions with $O(^3P)$, the values of T_A are1000 K, 2900 K and 1300 K for TCE, MeCl and MEK respectively[4,5]. From these values of T_A, it is clear that MeCl has a stronger temperature dependence than MEK. In order to achieve the high energy densities in Figures 8 and 9, the pulsed corona tube was operated at powers up to 30 W which resulted in the observed temperature increase. The strong temperature dependence of MeCl explains the increased removal at high energy densities in Fig. 9. Also, the slight increase in

removal efficiency of MEK in Fig. 8 at energy densities higher than 1500 J/l can now be seen to be attributed to this increase in gas temperature. Temperature effects were not seen in the measurements for TCE using the pulsed corona discharge since the powers necessary to achieve energy densities up to 400 J/l were very low (a few watts). The temperatures in the pulsed and ac-driven dielectric-barrier discharges always remained near room temperature.

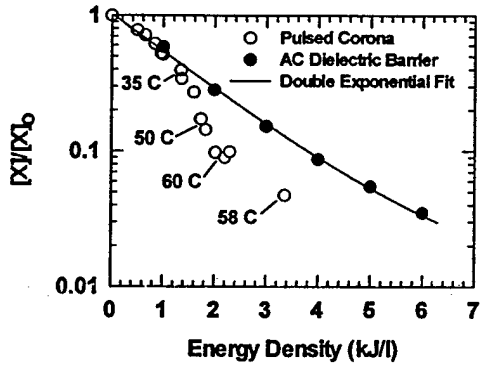

Figure 9. The removal versus energy density for 1000 ppm of MeCl in dry air.

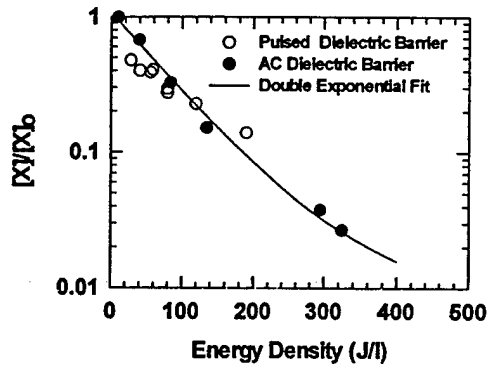

Figure 10. The removal versus energy density for 200 ppm of TCE in dry air.

The temperature effects on the removal of MeCl using the pulsed corona discharge are better illustrated under more controlled conditions as seen in Fig. 11. In this case the pulsed corona tube was externally heated by an oven. A large increase in removal efficiency is seen at elevated temperatures, a factor or 4 better removal at 150 C and a factor of 11 better removal at 250 C. Under these conditions, a quantity that cannot be ignored is the amount of thermal energy required to raise the gas to these temperatures. The added thermal energy in air, with respect to room temperature, is 180 J/l for 150 C and 300 J/l for 250 C. Even though the added thermal energy does not seem to be very significant with respect to the large decrease in discharge energy required to achieve a particular level of removal, it does indicate that there is an optimum temperature for a minimum total energy input to the system.

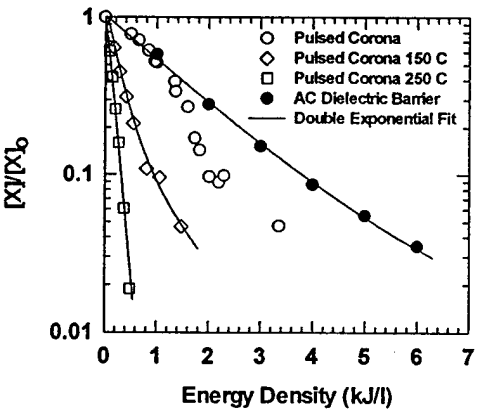

Figure 11. The removal versus energy density for 1000 ppm of MECL in dry air at various temperatures.

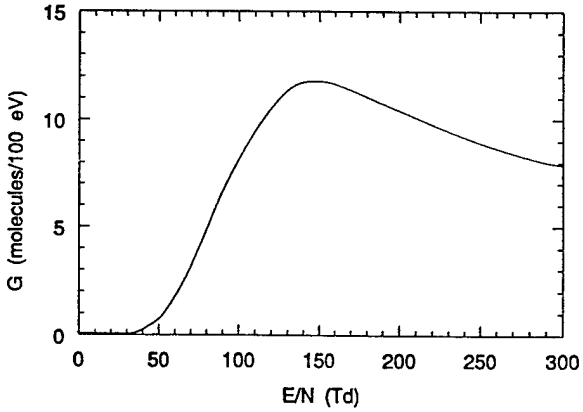

Figure 12. Typical G-value curve for O(^{3}P) radicals in dry air.

DISCUSSION

The breakdown voltage in the pulsed nonthermal plasma discharges is much larger than in a low-frequency ac-driven dielectric barrier discharge. The minimum voltage to produce a discharge in the pulsed corona tube was 12 kV for this wire and tube size, which, if only the geometry is taken in

consideration, produces an electric field of 120 kV/cm at the wire surface. The breakdown voltage in the pulsed dielectric-barrier discharge was 35 kV with a 2 mm air gap, which corresponds to an electric field of 130 kV/cm. The breakdown voltage in the ac-driven dielectric barrier cell was 7 kV at 1.2 kHz with a 3.5 mm air gap, which gives an electric field of 20 kV/cm. With such a large difference in breakdown electric field, it is reasonable to expect a difference in removal efficiency between the ac-driven and pulsed nonthermal plasma discharges. However, as seen in the data, there was no difference in removal efficiency between the different types of discharges at room temperature. To explain this, the reaction pathways leading to the destruction of these compounds must be investigated. For TCE, MEK, and MeCl in air it is well known that the initial chemical reaction is with the $O(^3P)$ radical produced in the discharge[2]. In that case, the production of $O(^3P)$ as a function of E/N, the reduced electric field strength which is related to the average electron energy in the discharge, is important. This is usually plotted as G versus E/N as seen in Fig. 12[1,6], where G is defined as the number of $O(^3P)$ radicals produced per 100 eV and E/N is in units of Townsends, Td, (where 1 Td = $1x10^{-17}$ V-cm^2). The values of breakdown E/N from the breakdown fields calculated above are 80 Td for the ac-driven dielectric-barrier discharge and approximately 500 Td for the pulsed discharges at room temperature and pressure. The two possible explanations for the same removal efficiencies at different breakdown fields are 1) the radical production happens to be approximately the same for the 80 Td discharge (to left of G vs E/N peak) and the 500 Td discharge (to right of the G vs E/N peak) or 2) the observed removal fractions (which correspond to radical formation efficiencies) suggest equivalent average conditions, where the radical formation is due more to an average value of E/N (or electron energy) which is approximately the same for these low-frequency or pulsed discharges.

CONCLUSIONS

A comparison has been made of the removal efficiency for three different nonthermal plasma reactors. A pulsed corona discharge and a low-frequency ac-driven dielectric-barrier discharge had similar removal efficiencies for TCE, MEK, and MECL in dry air at room temperature. Also, the removal efficiency was similar between both a pulsed and ac-driven dielectric barrier discharge for TCE in dry air at room temperature. Even though a large increase in breakdown field occurs in pulsed discharges, the similarity in removal efficiency can be explained if the chemical reaction pathways for these compounds in dry air are oxygen-atom-initiated. The change in removal efficiency with gas temperature is pronounced for MECL in air but has a weaker dependence for MEK in air which is consistent with the rate-constant temperature dependence found in the literature.

REFERENCES

1 *Non-Thermal Plasma Techniques for Pollution Control*, edited by B.M. Penetrante and S.E. Schultheis, Part A and Part B (Springer-Verlag, Berlin Heidelberg, 1993).

2 Z. Falkenstein, J. Adv. Oxidation Technology **1**, 1-16 (1997).

3 Y.L.M. Creyghton, E.M. Veldhuizen, and W.R. Rutgers, in *Non-Thermal Plasma Techniques for Pollution Control*, edited by B.M. Penetrante and S.E. Schultheis, Part A (Springer-Verlag, Berlin Heidelberg, pp. 205-230, 1992).

4 F. Westley, J.T. Herron, R.F. Hampson, W.G. Mallard, Editors, NIST Reference Database 17, National Institute of Standards and Technology, Gaithersburg, MD (1994).

5 P.Ott, D. Helf, and K. Kirchner, Dechema-Monographs **104**, 91-98 (1995).

6 J. Li, W. Sun, B. Pashaie, and S.K. Dhali, IEEE Trans. Plasma Sci. **23** (4), 672 (1995).